

Quantum pumping and rectification effects in Aharonov-Bohm-Casher ring-dot systems

F. Romeo, R. Citro and M. Marinaro

Dipartimento di Fisica "E. R. Caianiello", C.N.I.S.M. and NANOMATES

(Research Centre for NANOMaterials and nanotechnology),

Università degli Studi di Salerno, Via S. Allende, I-84081 Baronissi (Sa), Italy

We study the time-dependent transport of charge and spin through a ring-shaped region sequentially coupled to a weakly interacting quantum dot in the presence of an Aharonov-Bohm flux and spin-orbit interaction. The time-dependent modulation of the spin-orbit interaction, or of the corresponding Aharonov-Casher flux, together with the modulation of the dot-level induces an electrically pumped spin current even in absence of a charge current. The results beyond the adiabatic regime show that an additional rectification current proportional to $\cos(\varphi)$, being φ the relative phase between the time-varying parameters, is generated. We discuss the relevance of such term in connection with recent experiments on out-of-equilibrium quantum dots.

I. INTRODUCTION

In recent years the process of miniaturization of man-made electronic circuits has permitted to reach the molecular scale providing the opportunity of testing quantum mechanics in nano-electronics measurements¹. In this framework, one of the most exciting challenges is to encode information by means of the electron spin instead of the charge, giving rise to the so-called spin-based electronics or spintronics^{2,3}. To face the need of spin-polarizing systems acting as a source in spintronics devices, one promising possibility is to exploit the quantum interference effects by external electric or magnetic fields. In ring-shaped structures made of semiconducting materials a spin sensitive phase, the Aharonov-Casher phase⁶, is originated by the Rashba spin-orbit interaction^{4,5}. Such phase combined with the Aharonov-Bohm phase⁷ induced by a magnetic field is an useful tool to achieve spin-polarizing devices^{8,9}. Another interesting phase interference effect is originated by the periodic modulation of two out-of-phase parameters affecting the scattering properties of a nanostructure. Such phase effect, known in the literature as quantum pumping, was first introduced by Thouless¹⁰. After the Thouless theory, a scattering approach to the adiabatic quantum pumping was formulated by P. W. Brouwer¹¹ who showed that the d.c. current pumped by means of an adiabatic modulation of two out-of-phase independent parameters can be expressed in terms of the parametric derivatives of the scattering matrix. In the adiabatic regime described by the Brouwer formula, i.e. when the pumping frequency is much slower than the tunneling rates, a d.c. current proportional to $\sin(\varphi)$ is originated, being φ the phase difference between the two parameters. Such theoretical prediction has been verified experimentally by M. Switkes et al.¹² even though some anomalies in the current-phase relation have been reported. In particular, it has been observed a non-vanishing current at $\varphi = 0$. Several anomalies observed in the experiment can be explained by rectification of a.c. displacement currents as proposed in Ref.[13]. Ac-

cording to this work, the rectified currents are responsible for measurable effects which may be dominant over the pumping currents. In order to discriminate between rectified currents and pumping effects symmetry arguments can be exploited. For instance, the d.c. rectification voltage V_{rect} is symmetric under reversal of the magnetic field $V_{\text{rect}}(B) = V_{\text{rect}}(-B)$, while the voltage generated by a quantum pump is not. On the other hand, it has been shown in Ref.[14] that finite frequency effects, considered within a non-equilibrium Green's function approach, can lead to current-phase relations of the form $I_c = a \sin(\varphi) + b \cos(\varphi)$, where the coefficients a and b are function of the pumping frequency ω . Differently from the adiabatic regime where the pumped currents are odd function of the relative phase φ between the modulated parameters, any symmetry can be realized in the general non-equilibrium case.

In the following we analyze the charge and spin pumping in a ring-shaped conductor sequentially coupled to a quantum dot (see Fig.1) and apply the non-equilibrium Green's function approach to analyze the dc current from the adiabatic to non-adiabatic regime addressing the question about the existence of rectification terms. In the ring region shown in Fig.1 the electrons feel an Aharonov-Bohm phase associated to a time-varying Aharonov-Casher phase. The last is related to the Rashba spin-orbit interaction which is tunable by means of a gate voltage¹⁵. An additional time-dependent modulation of the dot energy level is also considered. If no voltage bias is present between the two external leads, the electron current is activated by absorption and emission of quantized photon energy. Thus, in the following the charge and spin pumped current are studied as a side-effect of boson-assisted tunneling.

The paper is organized as follows. In section II we introduce the model Hamiltonian and derive the general expression for the non-equilibrium Green's function and respective self-energies for the non-interacting and weakly interacting case. In section III, we employ a one-photon approximation and obtain a compact expression for the d.c. current pumped in the left lead. In section IV, we

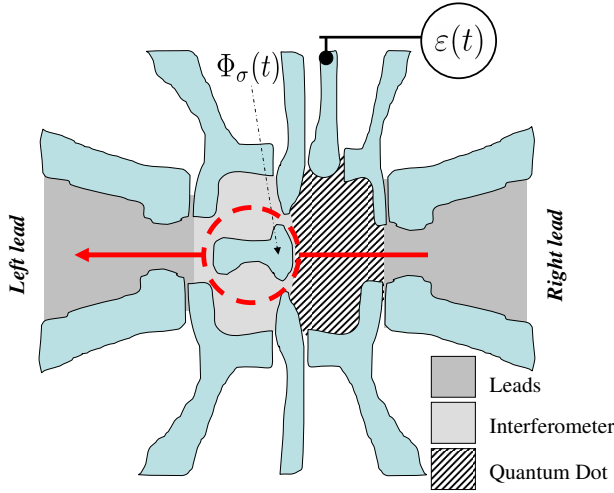
F
F
C

FIG. 1: An Aharonov-Bohm-Casher quantum ring sequentially coupled to a quantum dot. The energy on the dot and the Aharonov-Casher flux are modulated in time with frequency ω .

II. THE MODEL AND NON-EQUILIBRIUM CURRENT

The Hamiltonian of an Aharonov-Bohm-Casher ring sequentially coupled to an interacting quantum dot in the presence of time varying parameters can be written, in the local spin frame, as follows¹⁶:

$$H(t) = H_c + \sum_k \epsilon(t) d^\dagger_k d + U n_\uparrow n_\downarrow + \sum_k [2u \cos(\phi(t)) d^\dagger_k c_{k-1} + w c_{k+1}^\dagger d] + H_{\text{int}} \quad (1)$$

where $H_c = \sum_{k, \sigma} \epsilon_{k\sigma} c_{k\sigma}^\dagger c_{k\sigma}$ is the free electrons Hamiltonian describing the left/right ($l=r$) leads kept at the same chemical potential. The second and third term represent the dot Hamiltonian consisting of the electron-electron interaction term $U n_\uparrow n_\downarrow$ ($n_\sigma = d_\sigma^\dagger d_\sigma$) and of the time dependent dot energy level $\epsilon(t) = \epsilon_0 + \epsilon_1 \sin(\omega t + \phi)$, being ω the frequency of the modulation. The last term in Hamiltonian describes the tunneling between the left lead and the dot, $u \cos(\phi)$, and the right lead and the dot through a tunnel barrier, w . The transmission coefficients u and w , which in general may be spin and momentum dependent, are considered here constant for simplicity, i.e. $u = u(k = k_F)$ and $w = w(k = k_F)$, k_F being the Fermi momentum.

The electrons coming from the left lead acquire the time-dependent spin sensitive phase $\phi(t) = (\phi_{AB} + \phi_R(t))$ ($\phi_{AB} = \pi$), where ϕ_{AB} is the Aharonov-Bohm phase,

while ϕ_R is the Aharonov-Casher phase produced by the modulation of the Rashba spin-orbit interaction on the ring $\phi_R(t) = \phi_R^0 + \phi_R^1 \sin(\omega t)$ [9]. The Hamiltonian given in Eq.1 can be rewritten by means of a plane wave expansion in the following form:

$$H(t) = H_0 + \sum_l \sin(l\omega t + \phi) d^\dagger_l d + \sum_k [4u \cos(\phi_0) A(t) \sin(\phi_0) B(t) d^\dagger_k c_{k-1} + H_{\text{int}}] \quad (2)$$

where the static part H_0 of the Hamiltonian is the same as in Eq.(1) with: $\epsilon(t) \rightarrow \epsilon_0$, $u \rightarrow u J_0(\phi_R)$, $\phi_R(t) \rightarrow \phi_R^0$, while the functions $A(t)$ and $B(t)$ are given by (see APPENDIX A):

$$A(t) = \sum_{n=1}^{\infty} J_{2n}(\phi_R) \cos(2n\omega t) \quad (3)$$

$$B(t) = \sum_{n=1}^{\infty} J_{2n-1}(\phi_R) \sin((2n-1)\omega t); \quad (4)$$

where $J_n(x)$ are the Bessel functions of first kind. In absence of an external voltage, the quantum transport of particles through the structure is only due to absorption/emission of energy quanta $\hbar\omega$ associated to the external time-dependent fields.

To calculate the pumped current we employ the Keldysh Green's functions technique as formulated in Ref.[17]. The current in the left lead is given by $I_1(t) = \frac{e}{\hbar} \text{Tr}[\dot{H}_1 N_1]$ ($N_1 = \sum_k c_{k-1}^\dagger c_{k-1}$). It can be rewritten in terms of the retarded and lesser Green's functions $G^{r<}_0(t; t_1)$ and of the advanced/retarded self-energies $\Sigma^{a<}_1(t_1; t)$ of the quantum dot according to the following expression:

$$I_1(t) = \frac{e}{\hbar} \text{Tr}[\dot{H}_1 N_1] \quad (5)$$

$$I_1(t) = \frac{2e}{\hbar} \sum_{\sigma} \text{Ref} \int_{\sigma} dt_1 G^{r<}_0(t; t_1) \Sigma^{a<}_1(t_1; t) + \dots \quad (6)$$

For a time-dependent problem the retarded, advanced and lesser ($r, a, <$) Green's functions and respective self-energies depend explicitly on two time variables instead of one. Thus, employing the two time Fourier transform (see APPENDIX B) the current (5) can be rewritten as:

$$I_1(t) = \frac{2e}{\hbar} \sum_{\sigma} \text{Ref} \int \frac{dE_1 dE_2 dE_3}{(2\pi)^3} e^{i(E_3 - E_1)t} [G^{r<}_0(E_1; E_2) \Sigma^{a<}_1(E_2; E_3) + \dots] \quad (7)$$

where the lesser Green's function $G^{<}(E_1; E_2)$ of the dot is given by the Keldysh equation:

$$G^{<}(E_1; E_2) = \sum_{\sigma} \frac{d_1 d_2}{(2\pi)^2} G^{r<}(E_1; E_2) \Sigma^{a<}_1(E_2; E_3) \quad (8)$$

and the following relation between the retarded and advanced quantities can be used: $G^a(E_1; E_2) = [G^r(E_2; E_1)]^*$, where $G = G$ or f . In order to compute the current the knowledge of G^r , f^r , $f^<$ is required. Below we are going to calculate them for the non-interacting dot and the weakly interacting one. In both cases, the wide band limit (WBL) will be employed for simplicity.

A. Non-interacting case ($U = 0$)

In the $U = 0$ case the expression of the self-energies can be obtained exactly. By calling $w = u(2R)$, the retarded and lesser self-energies can be expressed in terms of the corresponding Green's functions of the leads, namely $G_k^r(t; t^0)_{sp} = i_{sp} \langle t - t^0 \rangle e^{i\epsilon_k(t - t^0)}$ and $G_k^<(t; t^0)_{sp} = i_{sp} f(\epsilon_k) e^{i\epsilon_k(t - t^0)}$, by the following relations:

$$\begin{aligned} G_{sp}^{r<}(t_1; t_2) &= \sum_{k; 2r} X \int_0^{2\pi} d\phi G_{kr}^{r<}(t_1; t_2)_{sp} + \\ &+ \sum_{k; 2l} X \int_0^{2\pi} d\phi \cos(\epsilon_s(t_1)) \cos(\epsilon_p(t_2)) G_{kl}^{r<}(t_1; t_2)_{sp} \end{aligned} \quad (9)$$

where s, p are spin indices (\uparrow, \downarrow), $f(\epsilon_k)$ is the Fermi function, while $\epsilon_k^1 = \epsilon_k^r = \epsilon_k$ in absence of voltage bias. In WBL limit and making the substitution $\epsilon_k = \epsilon_s + \epsilon_p$, we get:

$$\begin{aligned} G_{sp}^r(t_1; t_2) &= i_{sp} \langle t_1 - t_2 \rangle^0 [2 + 2 \cos^2(\epsilon_s(t_1))] \\ G_{sp}^<(t_1; t_2) &= i_{sp} f(t_1 - t_2)^0 [2 + 4 \cos^2(\epsilon_s(t_1))] \end{aligned} \quad (10)$$

where we introduced the quantities $\epsilon_s^0 = 2 \int_0^{2\pi} d\phi$ and $f(t_1 - t_2) = \frac{1}{2} f(\epsilon_s) e^{i\epsilon_s(t_1 - t_2)}$. By defining the left and right transition rates $\Gamma_s(t_1) = 2 \int_0^{2\pi} d\phi \cos^2(\epsilon_s(t_1))$ and $\Gamma_s^r(t_1) = 2 \int_0^{2\pi} d\phi \cos^2(\epsilon_s(t_1))$, the retarded self-energy can be written as $G_{sp}^r(t_1; t_2) = i_{sp} \langle t_1 - t_2 \rangle f(\Gamma_s(t_1) = 2 + \Gamma_s^r(t_1) = 2g)$ and thus the retarded Green's function of the quantum dot takes the following form¹⁸:

$$\begin{aligned} G_{sp}^r(t; t^0) &= G_{sp}^r(t; t^0) \exp \int_{t^0}^t dt_1 \left[\frac{1}{s}(t_1) + \frac{r}{s}(t_1) \right]; \\ G_{sp}^r(t; t^0) &= i_{sp} \langle t - t^0 \rangle \exp \int_{t^0}^t dt_1 \Gamma(t_1) \end{aligned} \quad (11)$$

It can be computed exactly after having performed the following plane-wave expansion of the retarded self-energy:

$$\begin{aligned} G_{sp}^r(t_1; t_2) &= i_{sp} \langle t_1 - t_2 \rangle^0 [1 + 2 + 2 \cos^2(\epsilon_s(t_1))] \\ &+ J_0(2 \int_0^{2\pi} d\phi) \cos(2 \int_0^{2\pi} d\phi) \\ &+ \cos(2 \int_0^{2\pi} d\phi) M(t_1) - s \sin(2 \int_0^{2\pi} d\phi) N(t_1) \end{aligned} \quad (12)$$

where the following auxiliary functions have been introduced:

$$M(t) = 2 \sum_{n=1}^{\infty} J_{2n}(2 \int_0^{2\pi} d\phi) \cos(2n! t) \quad (13)$$

$$N(t) = 2 \sum_{n=1}^{\infty} J_{2n-1}(2 \int_0^{2\pi} d\phi) \sin((2n-1)! t); \quad (14)$$

and whose Fourier transform is given by:

$$\begin{aligned} G_{sp}^r(E_1; E_2) &= i_{sp} f(E_1 - E_2) Q_1^s + \\ &+ i Q_2^s \sum_{n=1}^{\infty} J_{2n}(2 \int_0^{2\pi} d\phi) (E_1 - E_2 + 2n!) Q_3^s \\ &+ \sum_{n=1}^{\infty} J_{2n-1}(2 \int_0^{2\pi} d\phi) (E_1 - E_2 + (2n-1)!) g; \end{aligned} \quad (15)$$

An analogous plane-wave expansion can be performed for the lesser self-energy $G_{sp}^<(t_1; t_2)$, whose Fourier transform is the following:

$$\begin{aligned} G_{sp}^<(E_1; E_2) &= 2 i_{sp} f(E_1 - E_2) Q_1^s + \\ &+ \sum_{n=1}^{\infty} Q_2^s J_{2n}(2 \int_0^{2\pi} d\phi) f(E_1 + 2n!) (E_1 - E_2 + 2n!) + \\ &+ \sum_{n=1}^{\infty} i Q_3^s J_{2n-1}(2 \int_0^{2\pi} d\phi) f(E_1 + (2n-1)!) (E_1 - E_2 + (2n-1)!) g \end{aligned} \quad (16)$$

where Q_j^s are given by:

$$\begin{aligned} Q_1^s &= 2 \int_0^{2\pi} d\phi \cos^2(\epsilon_s(t_1)) = 2 + 1 + J_0(2 \int_0^{2\pi} d\phi) \cos(2 \int_0^{2\pi} d\phi) g \\ Q_2^s &= 2 \int_0^{2\pi} d\phi \cos(2 \int_0^{2\pi} d\phi) \\ Q_3^s &= 2 \int_0^{2\pi} d\phi \sin(2 \int_0^{2\pi} d\phi); \end{aligned} \quad (17)$$

The substitution of Eq.(16) and of $G^r(E_1; E_2)$ in Eq.(8) permits to determine the $G^<(E_1; E_2)$.

The knowledge of the retarded and lesser Green's function enables us to calculate the current generated by the pumping procedure in the form of a trigonometric series, i.e. $I_1(t) = I_0 + \sum_{n=1}^{\infty} [c_n \cos(n! t) + s_n \sin(n! t)]$, allowing to recognize the d.c. component of the current.

B. Weakly interacting case ($U \neq 0$)

The weakly interacting limit ($U \neq 0$) can be studied by means of a self-consistent Hartree-Fock theory which is known to give suitable results when the Coulomb interaction U is small^{20,21} (i.e., $U \ll \epsilon_s^0$). In this framework, the energy of the electrons on the dot is modified by a spin dependent term related to the occupation number of the electron of opposite spin and thus the spin dependent energy becomes $\epsilon(t) = \epsilon(t) + U h_n(t) i$ ($i = \uparrow, \downarrow$). The occupation number $h_n(t) i$ is calculated self-consistently by means of the relation $i h_n(t) i = G^<(t; t)$. The retarded Green's function of the dot is modified by the interaction according to the expression:

$$G_{sp}^r(t; t^0) = G_{sp}^r(t; t^0) \exp \int_{t^0}^t dt_1 i U h_s(t_1) i; \quad (18)$$

where $G_{sp}^r(t; t^0)$ represents the retarded Green's function derived in the non-interacting case. In order to determine the interacting Green's function, we can write $\ln_s(t_1)$ as a trigonometric series of $\sin(n!t)$, $\cos(n!t)$ with unknown coefficients calculated in a self-consistent way, as explained below.

III. THE SINGLE PHOTON APPROXIMATION

Hereon we focus on the weak pumping limit and consider only single photon processes, i.e. involving emission or absorption of a single energy quantum $\hbar\omega$. The weak pumping limit (i.e. the case in which a pure $\sin(\omega t)$ behavior of the current is expected) is very important in experiments where the higher harmonics contribution seem to be negligible even though other anomalies occur. Such anomalies in the current-phase relation will be discussed here later.

A. Non-interacting case ($U = 0$)

Within the single photon approximation the self-energies (15)–(16) can be approximated as:

$$\begin{aligned} \Sigma_{sp}^r(E_1; E_2) &= \sum_{\mathbf{X}} \text{sp} \text{fi}(E_1, E_2) Q_1^s + \\ &+ Q_3^s J_1(2\frac{\omega}{R}) (E_1 - E_2 - \omega) g \\ &= 1 \\ \Sigma_{sp}^<(E_1; E_2) &= \frac{2}{X} \text{sp} \text{fif}(E_1) Q_1^s - Q_3^s J_1(2\frac{\omega}{R}) \\ &\quad f(E_1 + \omega) (E_1 - E_2 + \omega) g \\ &= 1 \end{aligned} \quad (19)$$

The approximation is valid for small values of $2\frac{\omega}{R}$ so that the inequality $J_1(2\frac{\omega}{R}) \approx J_n(2\frac{\omega}{R})$, $n > 1$, is verified. Using the above approximated form of (19) the retarded Green's function of the quantum dot can be rewritten as follows:

$$\begin{aligned} G_{sp}^{r(1)}(t; t^0) &= \frac{i_{sp}}{n} (t - t^0) \\ &\quad \exp \left[i \left[\omega_0 - \frac{1}{2} Q_1^s \right] (t - t^0) \right] \\ &\quad \exp \left[i \int_{t^0}^t dt_1 \sin(\omega t_1) + \right. \\ &\quad \left. + \int_{t^0}^t dt_1 \cos(\omega t_1) \right]; \end{aligned} \quad (20)$$

where we introduced the coefficients:

$$\begin{aligned} \frac{s}{1} &= \omega_1 \cos(\omega t) + i J_1(2\frac{\omega}{R}) Q_3^s \\ \frac{s}{2} &= \omega_1 \sin(\omega t); \end{aligned} \quad (21)$$

and the upper index (1) stands for the single-photon approximation. Making a further expansion of the retarded Green's function for small $\omega_1 = \omega$ leads to the result:

$$G_{sp}^{r(1)}(t; t^0) \approx \frac{i_{sp}}{n} (t - t^0)$$

$$\exp \left[i \left[\omega_0 - \frac{1}{2} Q_1^s \right] (t - t^0) \right] \quad (22)$$

where $C(t; t^0) = \cos(\omega t) \cos(\omega t^0)$, $S(t; t^0) = \sin(\omega t) \sin(\omega t^0)$, while the coefficients $\frac{s}{j}$ have been defined as follows:

$$\begin{aligned} \frac{s}{0} &= J_0 \frac{\omega_1 \sin(\omega t)}{\omega_1} J_0 \frac{\omega_1 \cos(\omega t)}{\omega_1} \\ &\quad \frac{J_1(2\frac{\omega}{R}) Q_3^s}{\omega_1} \\ \frac{s}{1} &= 2 J_0 \frac{\omega_1^2}{\omega_1} I_0 \frac{\text{Im} f_{\frac{s}{1}g}}{\omega_1} J_0 \frac{\text{Re} f_{\frac{s}{1}g}}{\omega_1} \\ &\quad \frac{J_0 \frac{\text{Re} f_{\frac{s}{1}g}}{\omega_1} I_1 \frac{\text{Im} f_{\frac{s}{1}g}}{\omega_1} i J_1 \frac{\text{Re} f_{\frac{s}{1}g}}{\omega_1}}{\omega_1} \\ &\quad \frac{J_0 \frac{\text{Im} f_{\frac{s}{1}g}}{\omega_1} i}{\omega_1} \\ \frac{s}{2} &= 2 i I_0 \frac{\text{Im} f_{\frac{s}{1}g}}{\omega_1} J_0 \frac{\text{Re} f_{\frac{s}{1}g}}{\omega_1} J_1 \frac{\omega_1^2}{\omega_1} J_0 \frac{\omega_1^2}{\omega_1}; \end{aligned} \quad (23)$$

where $I_n(x)$ ($n = 0; 1$) represents the modified Bessel function of first kind and order n . The above result can be conveniently rewritten in terms of the two-time Fourier transform and thus we have:

$$\begin{aligned} G_{sp}^{r(1)}(E_1; E_2) &= 2 \sum_{\mathbf{X}} \frac{\frac{s}{0}(E_1, E_2)}{D^s(E_1)} + \\ &+ \sum_{\mathbf{X}} \frac{R^s(E_1, E_2 + \omega)}{D^s(E_1)(D^s(E_1) + \omega)}; \end{aligned} \quad (24)$$

where we defined $R^s = (\frac{s}{1} - i \frac{s}{2}) = 2$ and $D^s(E_1) = E_1 - \omega_0 + i Q_1^s = 2$. The knowledge of the retarded Green's function allows us to write the lesser Green's function by means of the Keldysh equation in this way:

$$\begin{aligned} G_{ss}^{<(1)}(E_1; E_2) &= 2 i Q_1^s F_s^0(E_1; E_2) + \\ &+ 2 Q_3^s J_1(2\frac{\omega}{R}) F_s(E_1; E_2); \end{aligned} \quad (25)$$

where we defined the following integral function:

$$\begin{aligned} F_s(E_1; E_2) &= \sum_{\mathbf{X}} \int_{t^0}^t \frac{d}{(2)^2} G_{ss}^{r(1)}(E_1; \omega) \\ &\quad f(\omega) G_{ss}^{r(1)}(E_2; \omega); \end{aligned} \quad (26)$$

The above function, disregarding terms quadratic in $J_1(x)$ and $I_1(x)$ and additional terms describing higher order processes (roughly cubic in $[D^s(E_1)]^{-1}$), can be written in the simple form:

$$F_s(E_1; E_2) = \frac{f(E_1 + \omega) [\frac{s}{0}]^2 (E_1, E_2 + \omega)}{D^s(E_1)(D^s(E_1) + \omega)}; \quad (27)$$

Thus, the d.c. current generated by the time-varying parameters has the following analytical expression:

$$hI_1^{s(1)}(t)i = \frac{eQ_1^s Q_1^s Q_0^s [1 - Q_0^s]}{h} \int_{-\infty}^{\infty} \frac{f(E) dE}{D^s(E) j^2} + \frac{2eQ_3^s J_1(2\frac{\omega}{R})}{h} \int_{-\infty}^{\infty} \frac{f(E) dE}{D^s(E) (D^s(E) + \omega^2)} g; \quad (28)$$

Here Q_1^s is a coefficient obtained setting $\omega = 0$ in Q_1^s (for the left lead). The current (28) contains terms proportional to ω^2 and $(\frac{\omega}{R})^2$ that can be interpreted as rectification terms, and terms proportional to $\omega \frac{\omega}{R}$ which contain information on the non-adiabatic pumping process, as will be clear below.

B. Weakly interacting case ($U \rightarrow 0$)

To perform the analysis in the weakly interacting case, we consider as negligible the terms proportional to U . In addition we also consider $U = \omega$ as a small quantity, being U of the same order of ω , $\frac{\omega}{R}$. Within the Hartree-Fock theory we need to determine the energy of the quantum dot $\epsilon(t) = \epsilon_0 + U n(t)$ with $n(t) = \langle n(t) \rangle$. By using the single photon approximation, we write the occupation number as a trigonometric series:

$$n(t) = a^{(0)} + a^{(1)} \sin(\omega t) + a^{(2)} \cos(\omega t); \quad (29)$$

where the unknown coefficients $a^{(i)}$ have to be determined self-consistently. In the interacting case the retarded Green's function takes the following form:

$$G_{sp}^{r(1)}(t; t^0) = \int_{-\infty}^{\infty} \frac{d\epsilon}{2\pi} \exp[-i(\epsilon_0 + U a_s^{(0)} - iQ_1^s/2)](t - t^0) \exp[-i \int_{t^0}^t d\tau_1 \sin(\omega \tau_1) + \int_{t^0}^t d\tau_1 \cos(\omega \tau_1)]; \quad (30)$$

where the coefficients a_i^s have been defined as follows:

$$\begin{aligned} a_1^s &= \omega \cos(\epsilon') + iJ_1(2\frac{\omega}{R})Q_3^s + U a_s^{(1)} \\ a_2^s &= \omega \sin(\epsilon') + U a_s^{(2)}; \end{aligned} \quad (31)$$

Note that since the coefficients $a_s^{(i)}$ appear as a factor of the interaction U , we have to calculate them only up to the zero order approximation in U and ω . From the lesser Green's function obtained by (30), we can write the occupation number in the following form:

$$n(t) = \frac{(\omega_0)^2}{2} [Q_1 - 2Q_3 J_1(2\frac{\omega}{R}) \sin(\omega t)] \int_{-\infty}^{\infty} \frac{f(E) dE}{D_0^s(E) j^2}; \quad (32)$$

where $D_0(E) = E - \epsilon_0 + iQ_1^s/2$. By comparing the above expression with the $G^{<(1)}(t; t)$ obtained by using (30) one gets the following set of self-consistency equations:

$$\begin{aligned} a^{(0)} &= \frac{Q_1}{2} \int_{-\infty}^{\infty} \frac{f(E) dE}{D_0^s(E) j^2} \\ a^{(1)} &= \frac{2Q_3}{Q_1} J_1(2\frac{\omega}{R}) a^{(0)} \\ a^{(2)} &= 0; \end{aligned} \quad (33)$$

Once the above equations are solved, the d.c. current can be written as in Eq.(28) with the following interaction-induced shift: $\epsilon_0 \rightarrow \epsilon_0 + U a^{(0)}$, $\frac{\omega}{R} \rightarrow \frac{\omega}{R} + U a^{(1)}$.

C. The spin and charge currents

To obtain an analytical expression of the d.c. current pumped in the left lead in the presence of a weak interaction and zero temperature, we need an approximated expression for R^s in (28) in the limit of $\frac{\omega}{R} \rightarrow 1$, and $2\frac{\omega}{R} \rightarrow 1$. In this limit one can use $J_1(x) \approx x/2$, $I_1(x) \approx x/2$, $J_0(x) \approx 1$, $I_0(x) \approx 1$ (see APPENDIX C) and thus the coefficients R^s take the following simplified form:

$$R^s = \frac{\omega \frac{\omega}{R} Q_3^s}{2!} + \frac{\omega \sin(\epsilon')}{2!} - \frac{i(\omega \cos(\epsilon') + U a_s^{(1)})}{2!}; \quad (34)$$

while the quantity $Q_0^s [1 - Q_0^s]$ can be written as follows:

$$Q_0^s [1 - Q_0^s] = \frac{1}{2} \frac{h \omega^2}{\omega^2} - \frac{(\omega \frac{\omega}{R} Q_3^s)^2}{\omega^2} + 2 \frac{a_s^{(1)} U \omega \cos(\epsilon')}{\omega^2} + O(\omega^4); \quad (35)$$

Plugging these expressions in (28) and performing the integral over the frequency, after an expansion up to the second order in ω , we can write the d.c. current in the single photon approximation (in units of $2^{-1} e \hbar$) as follows:

$$\begin{aligned} hI_1^{(1)}i &= \frac{q_i a^{(0)} h}{2!^2} \omega^2 [(2\frac{\omega}{R} q_3)^2 + 2a^{(1)} U \omega \cos(\epsilon') + \\ &\quad (q_3 \frac{\omega}{R})^2 \frac{h}{D(\omega)^2} \frac{\omega_0 + U(a^{(0)} - a^{(0)})}{j^2} + \\ &\quad + q_3 \frac{\omega \frac{\omega}{R} n \sin(\epsilon')}{2D(\omega)^2 j^2} [(\omega_0 - U a^{(0)})^2 - (q_1)^2] \\ &\quad + 2q_1 \cos(\epsilon')]; \end{aligned} \quad (36)$$

where the energies are measured in units of ϵ_0 , while we defined $q_i = Q_i - Q_0$. The non-dimensional charge and spin currents, i.e. I_c and I_s , can be defined as $I_c = \frac{I_c}{e}$ and $I_s = \frac{I_s}{e}$. The main feature of the expression for the d.c. current is the presence of

a non-sinusoidal current-phase relation already in weak-pumping. Indeed, contrarily to the adiabatic case characterized by a current-phase relation with definite odd parity (i.e. $I_c(\varphi) = -I_c(\varphi + \pi)$) in the time-dependent case any parity with respect to the sign reversal of φ is expected in the pumped current. This behavior is mainly related to finite frequency effects as well as to interaction effects. Eq.(36) represents the main result of this work.

IV. NUMERICAL RESULTS AND DISCUSSION

In order to make a comparison with the available experimental data, we set $\mu_0 = 10$ eV [22]. Such quantity is related to the dwell time τ_d by the following relation $E = \hbar/\tau_d = 2\mu_0$. Such quantity is relevant to define the various transport regimes at varying frequency ω . Indeed, for value of $\omega \tau_d \ll 1$ one deals with the adiabatic regime, while in the opposite limit, i.e. $\omega \tau_d \gg 1$, the non-adiabatic regime is approached. For typical experimental frequencies ranging from 10 MHz up to 20 GHz, $\omega \tau_d$ varies from 10^{-2} up to order 10 and thus the MHz range of frequency can be safely considered as adiabatic. The adimensional frequency ω which appears in Eq.(36) is defined as $\omega = \hbar\omega/\mu_0 = \omega \tau_d$. In this way a frequency of 25 MHz corresponds to $\omega = 0.01$, 100 MHz to $\omega = 0.04$, 1 GHz to $\omega = 0.4$. In the following we study the behavior of charge and spin currents in the range of frequency $\omega \in [0.1; 0.5]$, thus our analysis is valid from adiabatic up to the moderate non-adiabatic limit. We also set the chemical potential as the zero of energy. From the analysis of the current i , we notice the presence of two classes of terms contributing to the currents: 1) Terms proportional to μ_0^2 or $(\mu_R/\mu_0)^2$; 2) terms proportional to $\mu_R \mu_0$. The first type of terms are non-adiabatic in nature. The second class of terms contains a term proportional to ω , which can be recognized as the quantum pumping contribution, and a frequency independent term proportional to $\cos(\varphi)$ which can be interpreted as a rectification contribution. Such term is responsible for the non-sinusoidal behavior that leads to an anomalous current-phase relation as observed in Ref.[22] (page 3, first column, line 2). Very interestingly, the interaction effects also lead to a cosine term which is proportional to $U \mu_R \cos(\varphi) = \omega^2$. Such a term produces a deviation from the sinusoidal behavior also for small values of the energy U . Finally, the current i vanishes when the amplitude of the modulation μ_R and μ_R/μ_0 go simultaneously to zero.

In Fig.2 the charge (dashed-dotted line) and spin (full line) currents, namely I_c and I_s , as a function of the phase difference φ between the time-varying parameters are reported for the following choice of parameters: $\omega = 0.05$, $\mu_{AB} = 0.49$, $\mu_R^0 = 0.02$, $\mu_R^1 = 0.01$, $\mu_0 = 0$, $\mu_1 = 0.025$, $\omega = 0.1$ and $U = 0$. A sinusoidal-like behavior is observed even though the charge pumped for $\varphi = 0$ is different from zero and of the order 10^{-3} . This

is a fingerprint of the anomalous current-phase relation, as discussed above. To put in evidence the dependence

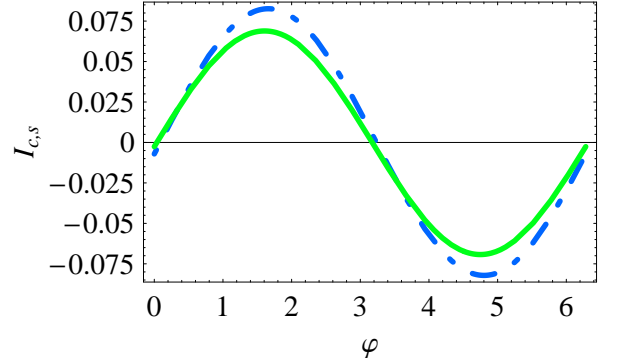


FIG. 2: Currents of charge (dashed-dotted line) and spin (full line) as a function of φ obtained for the following choice of parameters: $\omega = 0.05$, $\mu_{AB} = 0.49$, $\mu_R^0 = 0.02$, $\mu_R^1 = 0.01$, $\mu_0 = 0$, $\mu_1 = 0.025$, $\omega = 0.1$ and $U = 0$.

on the interaction U , we present in Fig.3 the charge current computed at $\varphi = 0$ (dashed line) and $\varphi = \pi/2$ (full line) as a function of U taking the remaining parameters as in Fig.2. Smaller values of the interaction favours deviation from the sinusoidal behavior. Below we con-

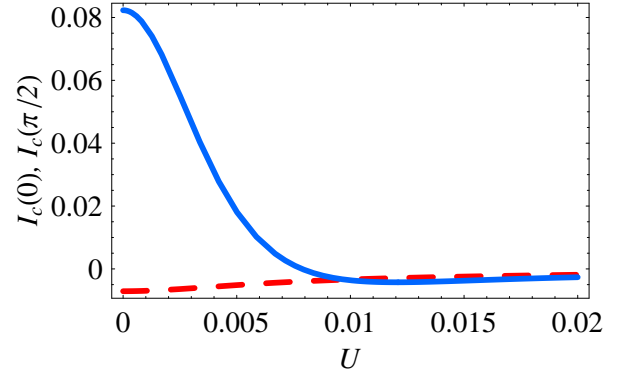


FIG. 3: Currents of charge computed at $\varphi = 0$, $I_c(\varphi = 0)$ (dashed line), and $\varphi = \pi/2$, $I_c(\varphi = \pi/2)$ (full line), as a function of U obtained for the following choice of parameters: $\omega = 0.05$, $\mu_{AB} = 0.49$, $\mu_R^0 = 0.02$, $\mu_R^1 = 0.01$, $\mu_0 = 0$, $\mu_1 = 0.025$, $\omega = 0.1$.

centrate on the role of spin-orbit interaction and choose the Aharonov-Bohm flux close to half integer values in unit of the flux quantum $\phi_0 = \hbar/e$ where the charge current is activated by photon-assisted tunneling (PAT). Away from the above values of the Aharonov-Bohm flux the currents present an oscillating behavior as a function of the applied magnetic flux μ_{AB} similar to the one already discussed in a previous work²³.

In Fig.4 we plot I_c (dashed-dotted line) and I_s (full line) as a function of the static Aharonov-Casher phase μ_R^0 for pumping frequency $\omega = 0.2$, $\omega = 0.3$, $\omega = 0.4$ (from top to bottom) and by setting the remaining parameters as

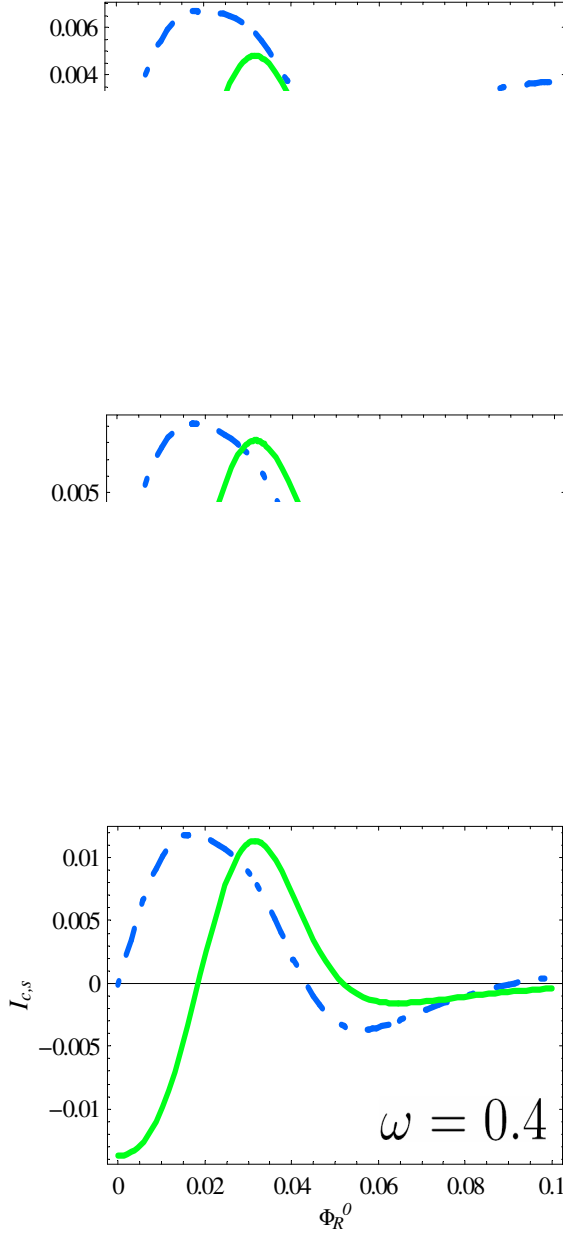


FIG. 4: Charge (dashed-dotted line) and spin (full line) currents as a function of Φ_R^0 obtained for the following choice of parameters: $\epsilon = 0.05$, $\alpha_{AB} = 0.49$, $\beta_R = 0.01$, $\mu_0 = 0.025$, $\mu_1 = 0.05$, $\gamma = 5$, $\omega = 4$, $U = 0$. The upper panel is obtained for $\omega = 0.2$, the middle panel for $\omega = 0.3$ and the lower panel for $\omega = 0.4$.

frequency from $\omega = 0.2$ (500 MHz) up to 0.4 (1 GHz) zeros of the charge currents start to appear and thus it is possible to obtain pure spin currents in the non-adiabatic regime. It is worth mentioning that currents of amplitude 10^{-2} in dimensionless units correspond to 50 pA in dimensional unit, thus the pure spin current we find is sizable.

To analyze the role of a weak Coulomb interaction, we plot in the upper panel of Fig. 5 the charge and spin currents for the same parameters as in Fig. 4 ($\omega = 0.3$) and by setting $U = 0.02$. A qualitatively different behavior of the charge current as a function of the Aharonov-Casher flux is observed. In particular, when the interaction en-

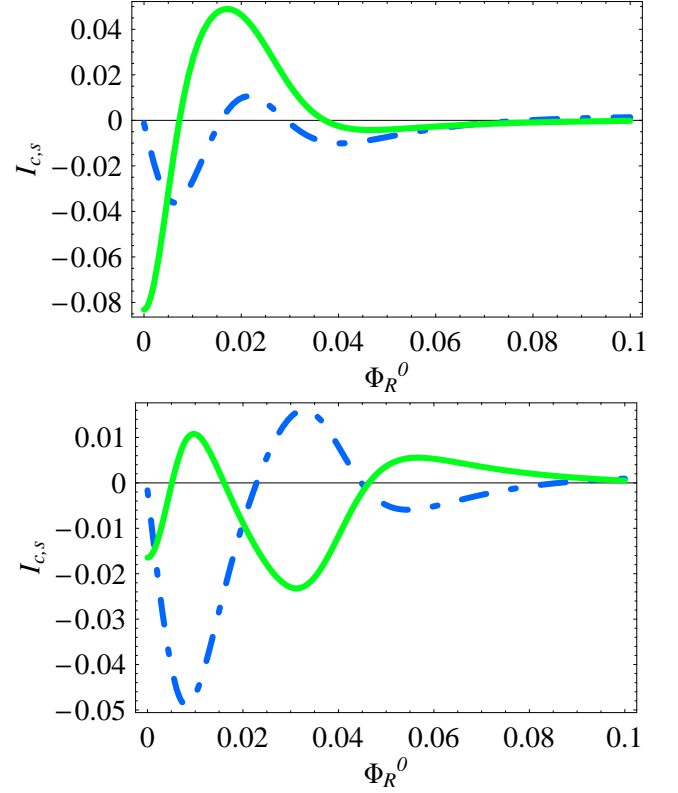


FIG. 5: Charge (dashed-dotted line) and spin (full line) currents as a function of Φ_R^0 obtained for the following choice of parameters: $\epsilon = 0.05$, $\beta_R = 0.01$, $\mu_0 = 0.025$, $\mu_1 = 0.05$, $\gamma = 5$, $\omega = 4$, $\omega = 0.3$, $U = 0.02$ and $\alpha_{AB} = 0.49$ in the upper panel, $\alpha_{AB} = 0.52$ in the lower panel.

ergy U is of the same order of magnitude of the pumping frequency ω , additional zeros of the charge current appear and this is a very appealing situation for spintronics devices. For instance, looking at Fig. 5 (upper panel), one observes a pure spin current close to $\Phi_R^0 = 0.015$ and 0.03 .

In the lower panel of Fig. 5 we plot charge and spin currents as done in the upper panel and by setting the Aharonov-Bohm flux to $\alpha_{AB} = 0.52$. In this case, a characteristic oscillating behavior of the currents controlled by using a magnetic flux is visible.

Another interesting phenomenon is the asymmetric contribution to the current of the photon absorption and emission as a function of the dot level μ_0 , as also reported in Ref. [24]. When the dot level lies above the Fermi level ($\mu_0 > 0$), an electron on the dot can jump in the left lead by emitting a photon. For $\mu_0 < 0$, an electron on the dot can reach the left lead only by means of the absorption of a photon since no voltage bias or temperature

gradient are present. Because of the interference between these two-photon sources, boson-assisted tunneling onto the dot gets suppressed while tunneling out of the quantum dot is enhanced. The asymmetric behavior of the d.c. current as a function of the dot level is shown in Fig.6. In the upper panel, we plot the charge current I_c

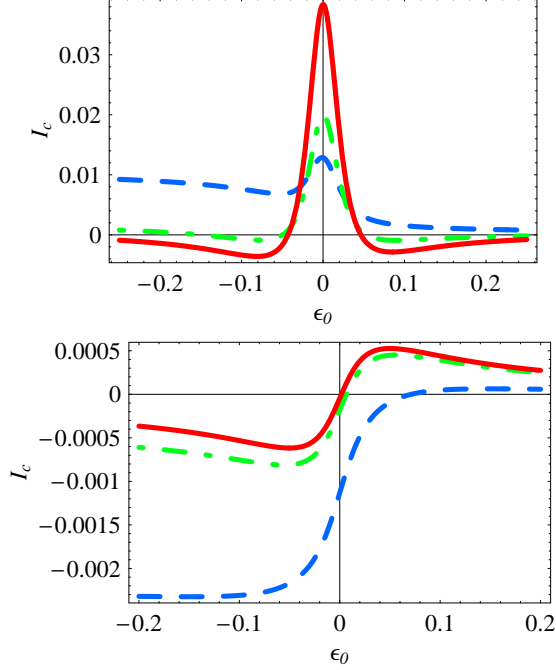


FIG. 6: Charge current I_c as a function of ϵ_0 obtained for the following choice of parameters: $\epsilon_0 = 0.05$, $\epsilon_{AB} = 0.49$, $\epsilon_R^0 = 0.05$, $\epsilon_R^1 = 0.01$, $\phi' = \pi/2$, $U = 0$ and $\epsilon_L^1 = 0.05$ for upper panel, $\epsilon_L^1 = 0$ for lower panel. Each panel contains curves obtained for $\omega_L = 0.1$ (dashed line), $\omega_L = 0.25$ (dashed-dotted line), $\omega_L = 0.5$ (full line).

as a function of the dot level ϵ_0 and by setting the remaining parameters as: $\epsilon_0 = 0.05$, $\epsilon_{AB} = 0.49$, $\epsilon_R^0 = 0.05$, $\epsilon_R^1 = 0.01$, $\phi' = \pi/2$, $U = 0$ and $\epsilon_L^1 = 0.05$. As can be seen, when the frequency ω_L is increased from 0.1 (dashed line) up to 0.5 (full line) a strong peak is formed at Fermi energy and the asymmetry of the current with respect to the $\epsilon_0 = 0$ becomes more evident. It is worth to mention that, since the relative phase ϕ' is $\pi/2$, all the terms in the current proportional to $\cos(\phi')$ are suppressed, while the pumping term takes its maximum value. In the lower panel we set $\epsilon_L^1 = 0$, while the remaining parameters are fixed as in the upper panel. In this case the device works as a single-parameter pump associated to the Aharonov-Casher flux and the current is proportional to $(\epsilon_R^1)^2$. A comparison between the upper and the lower panels shows that the pumping mechanism is the dominant one at the Fermi energy. Furthermore, we have verified that a small interaction does not alter too much the picture given so far.

The same analysis performed in Figs.6 can be repeated by setting $\phi' = 0$ to include the $\cos(\phi')$ contribution. In

the upper panel of Fig.7 we plot the current obtained for $\epsilon_L^1 = 0.05$, while in the lower panel this parameter is set to zero (single-parameter pump). By comparing

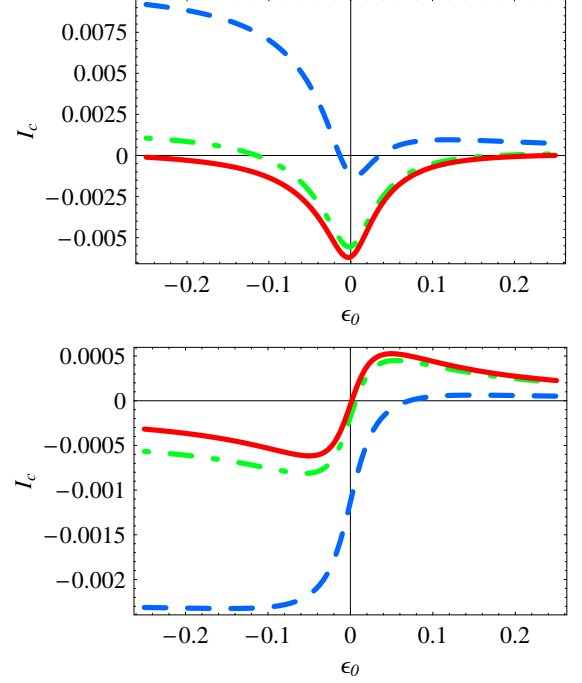


FIG. 7: Charge current I_c as a function of ϵ_0 obtained for the following choice of parameters: $\epsilon_0 = 0.05$, $\epsilon_{AB} = 0.49$, $\epsilon_R^0 = 0.05$, $\epsilon_R^1 = 0.01$, $\phi' = 0$, $U = 0$ and $\epsilon_L^1 = 0.05$ for upper panel, $\epsilon_L^1 = 0$ for lower panel. Each panel contains curves obtained for $\omega_L = 0.1$ (dashed line), $\omega_L = 0.25$ (dashed-dotted line), $\omega_L = 0.5$ (full line).

the results, one observes an enhancement of the absolute value of the high frequency currents in the case of double-parameter modulation (upper panel) and close to the Fermi energy.

From the analysis above one observes that, within the considered parameters region, the dominant mechanism for the generation of the d.c. current is the finite frequency quantum pumping. Indeed, close to the Fermi energy such currents take values which range from 70pA up to 190pA (see the upper panel of Figs.6), while in the other cases the generated currents present values of about 10% of those induced by the pumping process. Thus, for ϵ_{AB} close to half-integer values the quantum pumping induces the main contribution to the current, while away from this flux region the rectification currents are dominant.

V. CONCLUSIONS

We studied the time-dependent charge and spin transport (pumping) in a Aharonov-Bohm-Casher ring sequentially coupled to a weakly interacting quantum dot by using a non-equilibrium Green's function approach.

By varying a considerable number of parameters, we showed that the proposed device can work as a spin current generator and analyzed all its characteristics, including rectification effects. When the energy level $\epsilon(t)$ on the dot and the Aharonov-Casher flux are periodically modulated in time with a frequency Ω , a d.c. current is observed in the leads. Contrarily to the adiabatic case, the current-phase relation presents two additional cosine terms: The first one comes from the interaction on the dot, while the second can be interpreted as a rectification effect, as already noted in Ref.[22]. We also showed that Coulomb interaction effects can enhance the rectification effects. As a function of the spin-orbit interaction and close to the non-adiabatic regime, the results of the charge current show the appearance of additional zeros at varying the Aharonov-Casher flux. Thus, the finite frequency regime close to 750 MHz ($\Omega = 0.3$) is suitable to obtain pure spin currents useful in spintronics. Such currents are of the order of magnitude of 100pA as detected in the experiments on quantum dots²⁵. Finally, the analysis as a function of the dot level showed a characteristic asymmetric behavior and the comparison between the single parameter pump and double-parameters one showed a considerable increase of the d.c. current in the second case. The proposed device can be easily fabricated on a GaAs/AlGaAs two-dimensional electron gas using e-beam lithography to define the ring and dot region modifying, for instance, the system studied in Ref.[25].

ACKNOWLEDGMENTS

One of the authors (F.R.) would like to honor the memory of Antonio Calderaro who prematurely terminated his human adventure when the authors were writing this work.

APPENDIX A: BESSEL EXPANSION

Throughout the paper the following expansions have been exploited:

$$\sin(x \sin(\theta)) = 2 \sum_{n=1}^{\infty} J_{2n-1}(x) \sin((2n-1)\theta)$$

$$\begin{aligned} \cos(x \sin(\theta)) &= J_0(x) + 2 \sum_{n=1}^{\infty} J_{2n}(x) \cos(2n\theta) \\ \exp[i \cos(\theta)] g &= \sum_{n=-\infty}^{\infty} I_n(x) \exp(in\theta): \end{aligned} \quad (A1)$$

APPENDIX B: TWO-TIME FOURIER TRANSFORM

The two-time Fourier transform has been defined according to the following definitions:

$$\begin{aligned} g(t_1; t_2) &= \int_{-\infty}^{\infty} \frac{dE_1}{2} \frac{dE_2}{2} \\ &\quad g(E_1; E_2) \exp[-iE_1 t_1 + iE_2 t_2] \\ g(E_1; E_2) &= \int_{-\infty}^{\infty} dt_1 dt_2 g(t_1; t_2) \exp[iE_1 t_1 - iE_2 t_2] \end{aligned} \quad (B1)$$

APPENDIX C: APPROXIMATION OF $J_0(x)$, $J_1(x)$, $I_0(x)$, $I_1(x)$ FOR $x \ll 1$.

Throughout the paper the following approximations have been exploited:

$$\begin{aligned} J_0(x) &\approx 1 - \frac{x^2}{4} + O(x^4) \\ J_1(x) &\approx \frac{x}{2} + O(x^3) \\ I_0(x) &\approx 1 + \frac{x^2}{4} + O(x^4) \\ I_1(x) &\approx \frac{x}{2} + O(x^3): \end{aligned} \quad (C1)$$

¹ R.Hanson et al, Rev.Mod.Phys. 79, 1217 (2007).

² D.D.Awschalom, D.Loss, and N.Samarth, eds., Semiconductor Spintronics and Quantum Computation (Springer, Berlin, 2002).

³ I.Zutic, J.Fabian, and S.D.Sarma, Rev.Mod.Phys. 76, 323 (2004).

⁴ E.I.Rashba, Sov.Phys.Solid State 2, 1109 (1960).

⁵ Y.A.Bychkov and E.I.Rashba, J.Phys.C 17, 6039 (1984).

⁶ Y.Aharonov and A.Casher, Phys. Rev. Lett. 53, 319 (1984).

⁷ Y.Aharonov and D.Bohm, Phys.Rev.115, 485 (1959).

⁸ J.Splettstoesser, M.Govemare and U.Zuelicke, Phys.Rev.B 68, 165341 (2003).

⁹ D.Frustaglia, M.Hentschel, and K.Richter, Phys.Rev.B 69, 155327 (2004).

¹⁰ D.J.Thouless, Phys.Rev.B 27, 6083 (1983).

¹¹ P.W.Brouwer, Phys.Rev.B 58, R10135 (1998).

¹² M.Switkes, C.M.Marcus, K.Campman and A.C.Gossard, Science 283, 1905 (1999).

¹³ P.W.Brouwer, Phys.Rev.B 63, 121303(R) (2001).

- ¹⁴ B. Wang, J. Wang and H. Guo, *Phys. Rev. B* **65**, 073306 (2002).
- ¹⁵ J. Nitta et al., *Phys. Rev. Lett.* **78**, 1335 (1997).
- ¹⁶ Notice that the Hamiltonian model proposed in this work is the time dependent version of the one analyzed in *Phys. Rev. B* **77**, 193309 (2008).
- ¹⁷ A. P. Jauho, N. S. Wingreen and Y. Meir, *Phys. Rev. B* **50**, 5528 (1994).
- ¹⁸ D. C. Langreth and P. Nordlander, *Phys. Rev. B* **43**, 2541 (1991).
- ¹⁹ R. Aguado and D. C. Langreth, *Phys. Rev. Lett.* **85**, 1946 (2000); see also B. H. Wu and J. C. Cao, *Phys. Rev. B* **77**, 233307 (2008).
- ²⁰ H. Bruus and K. Flensberg, *Many Body Quantum Theory in Condensed Matter Physics: An Introduction* (Oxford University Press, Oxford, 2004).
- ²¹ S. Doniach and E. H. Sondheimer, *Green's Functions for Solid State Physicists* (Imperial College, London, 2004).
- ²² L. D'Carlo, C. M. Marcus and J. S. Harris Jr., *Phys. Rev. Lett.* **91**, 246804 (2003).
- ²³ R. Citro and F. Romeo, *Phys. Rev. B* **73**, 233304 (2006).
- ²⁴ M. Braun and G. Burkard, *Phys. Rev. Lett.* **101**, 036802 (2008).
- ²⁵ S. K. Watson, R. M. Potok, C. M. Marcus and V. Umansky, *Phys. Rev. Lett.* **91**, 258301 (2003).